PROCEEDINGS

OF THE

FIFTH SYMPOSIUM

ON THE

GEOLOGY OF THE BAHAMAS

Edited by

Roger J. Bain

Production Editor

Donald T. Gerace

Bahamian Field Station
San Salvador, Bahamas
1991

Printed in USA by Don Heuer

ISBN 0-935909-37-0

USE OF GRAVITY TECHNIQUES TO DETECT SHALLOW CAVES ON SAN SALVADOR ISLAND, BAHAMAS

A.W. Gerhard Kunze
Department of Geology
The University of Akron
Akron, Ohio 44325

John E. Mylroie
Department of Geology and Geography
Mississippi State University
Mississippi State, Mississippi 39762

ABSTRACT

Pleistocene sea level high stands produced dissolution conduits on San Salvador Island, Bahamas. Elevation of the freshwater lens by the sea level high stands resulted in mixing-zone dissolution where the lens thinned at the margin of the island. The resulting caves formed without human-sized opening to either the ocean or the land surface. Under today's sea level conditions, the caves are drained and abandoned. They are recognized only where surface erosion has breached into them in a random pattern suggesting that many caves exist that have no accessible connection to the surface, and are therefore unknown.

Two gravity traverses were run over Garden Cave, San salvador Island, Bahamas, to see if gravity data could allow the recognition of a subaerial cave passage of known depth and configuration. Station spacing was 4.6 m (15 feet) on traverses roughly perpendicular to the trend of the cave. The instrument used was a Worden (Master model) gravimeter. The cave produces negative gravity anomalies of close to 100 microgals, superimposed on a strong NNE regional trend. Gravity techniques can detect caves in this setting, but the logistics of gravity surveying preclude its use as a general reconnaissance tool for cave location. At specific areas, such as construction sites, it can be used to test for shallow, subaerial voids in the Bahamas.

INTRODUCTION

Subsurface cavities represent potential hazards to surface structures or engineering works. Potentially dangerous shallow dissolution caves are abundant throughout the Bahama Islands (Mylroie, 1988). These caves developed during a past, high sea level(s) when the freshwater lens was elevated to a position above current sea level. The majority of these caves are developed in rock 150,000 years old or less. They are found at elevations of 0 to +6 m above modern sea level. The caves must have developed during the high sea level events associated with oxygen isotope substages 5e, 5c and 5a (Shackleton and Opdyke, 1973) as those events are the only ones younger than the rocks which contain the caves. The sea level high stand associated with substage 5e has been demonstrated world-wide to have reached high enough above modern sea level. The data supporting high stands at substages 5c and 5a is still under debate (Carew and Mylroie, 1987; Mylroie and Carew, 1988; Vacher and Hearty, 1989; Lundberg, 1990).

The caves formed rapidly in the mixing zone found in the distal end of discharging fresh or brackish-water lenses under small, isolated dune ridges. They have formed in a unique manner, called the "flank margin model" (Mylroie and Carew, 1990, Vogel and others, 1990), which produces phreatic chambers with a maze-like character. The caves did not function as true conduits, but formed as mixing chambers inside the dunes. They have no natural entrance to the surface. The abandoned caves entered today have been breached by surface erosion such as scarp retreat and vadose shaft development. The distribution of the caves (Figure 1) suggests many more caves exist than have been located. The unlocated caves for the most part

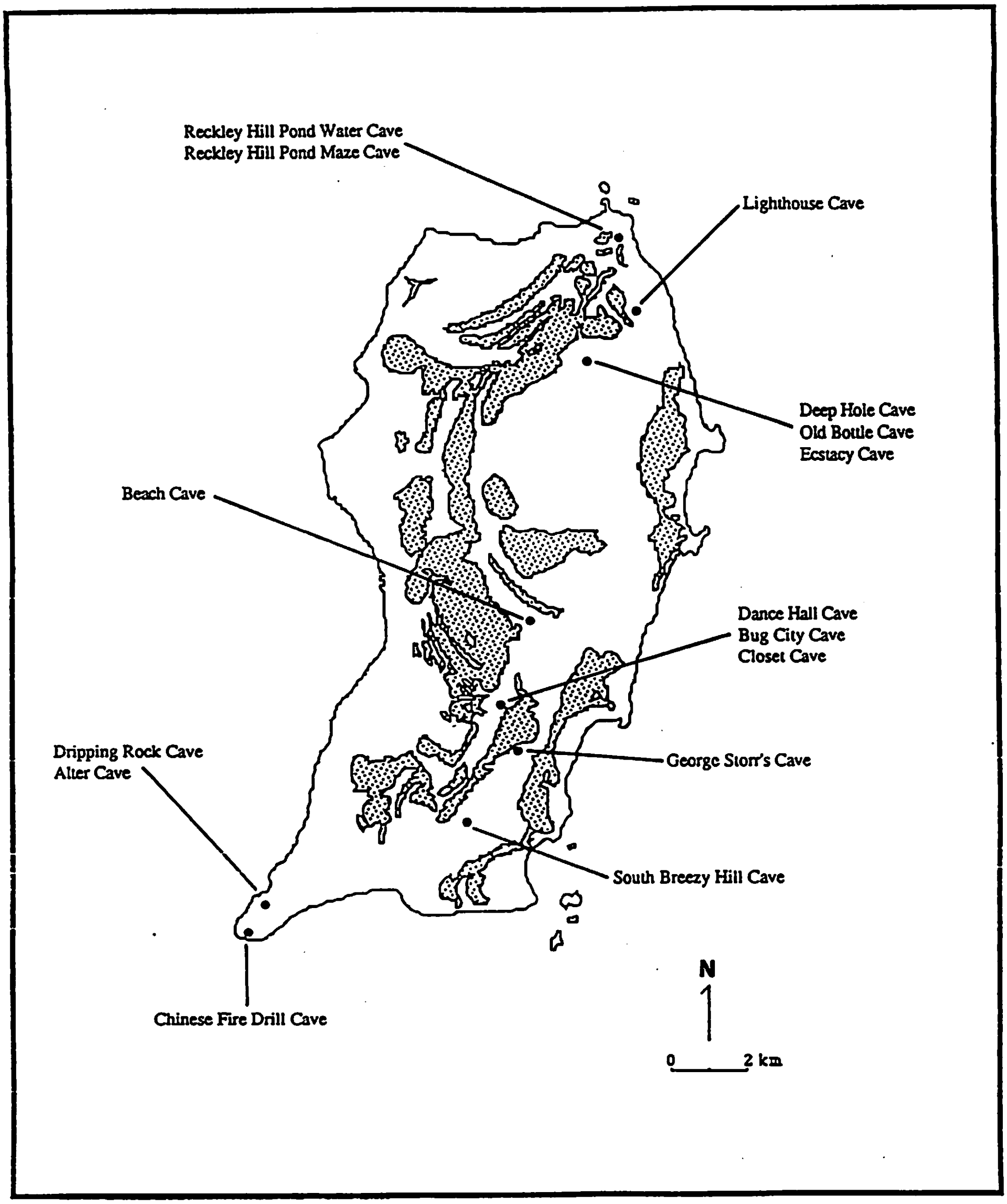

1. Locations of mapped solution caves on San Salvador Island, Bahamas, in addition to Garden Cave.

have not yet been opened to the surface. The purpose of this paper is to report on the success of using a gravimeter to locate caves which otherwise would be undetectable because they have no entrance.

Microgravity surveys are generally accepted engineering geophysical methods of locating and mapping shallow subsurface cavities. The missing mass represented by typical flank margin dissolution caves of 1-2m height should result in negative gravity anomalies on the order of 100 microgal, depending on rock densities and depth of the cave below the surface. Anomalies of that magnitude can be reliably detected and mapped using a Worden gravimeter. However, inversion of the resulting gravity data is not unique and is based on various assumptions concerning density, cave depth and cave geometry. Consequently, the calculated cave models may be incorrect. To evaluate the applicability of the microgravity method for cave detection and mapping in the Bahamas, a gravity test survey was conducted over Garden Cave, a shallow cave of known dimensions on San Salvador Island, using a Worden gravimeter.

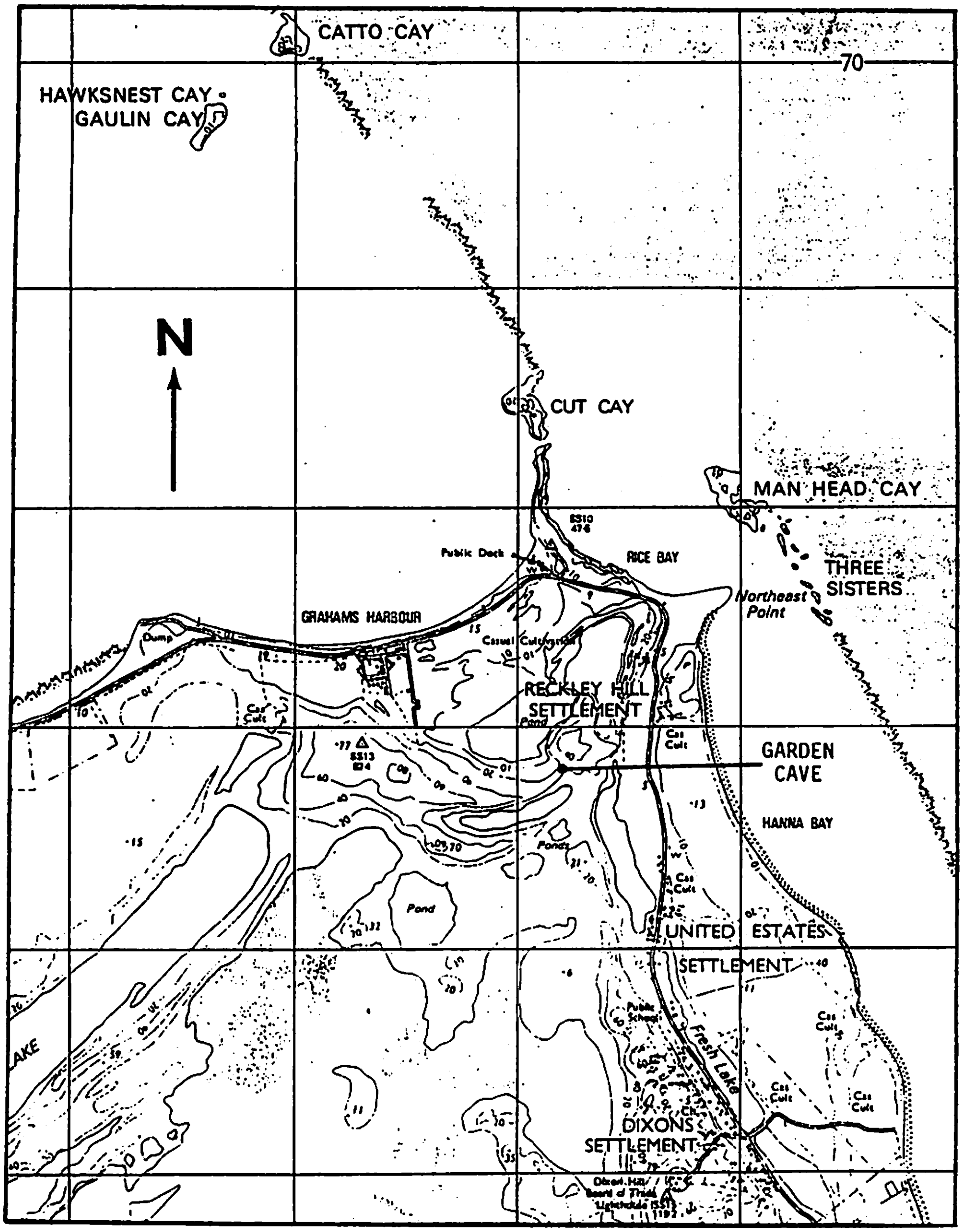

2. Location map for Garden Cave. The cave is just south and slightly east of the Reckley Hill Pond caves shown in figure 1. UTM grid spacing is 1 km.

METHODOLOGY

Garden Cave (see Figures 2 and 3) was chosen for this study because it represents a typical flank-margin cave undergoing destruction by surface erosion processes. At its northwest end, the cave is essentially intact. Moving to the southeast, then east, the cave is progressively more destroyed, until only open depressions and cave fragments exist. The cave was surveyed with compass and tape in December 1989 and January 1990.

Two gravity traverses were run over Garden Cave along two survey lines cut into the dense bush, about 60m long and roughly perpendicular to the trend of the cave; another gravity traverse was run along the axis of the cave (see Figure 4). Twenty-eight stations, spaced about 4.6m apart along the two perpendicular profiles and 10m along the longitudinal profile, were established. Relative station elevations were determined by transit to within 5cm. At least two gravity measurements were taken at each station with a Worden Master model gravimeter (Ser. No. 953) from the University of Akron. If the two gravity measurements disagreed, one to three additional readings were taken (at most stations). Traverse 1 gravity was measured twice

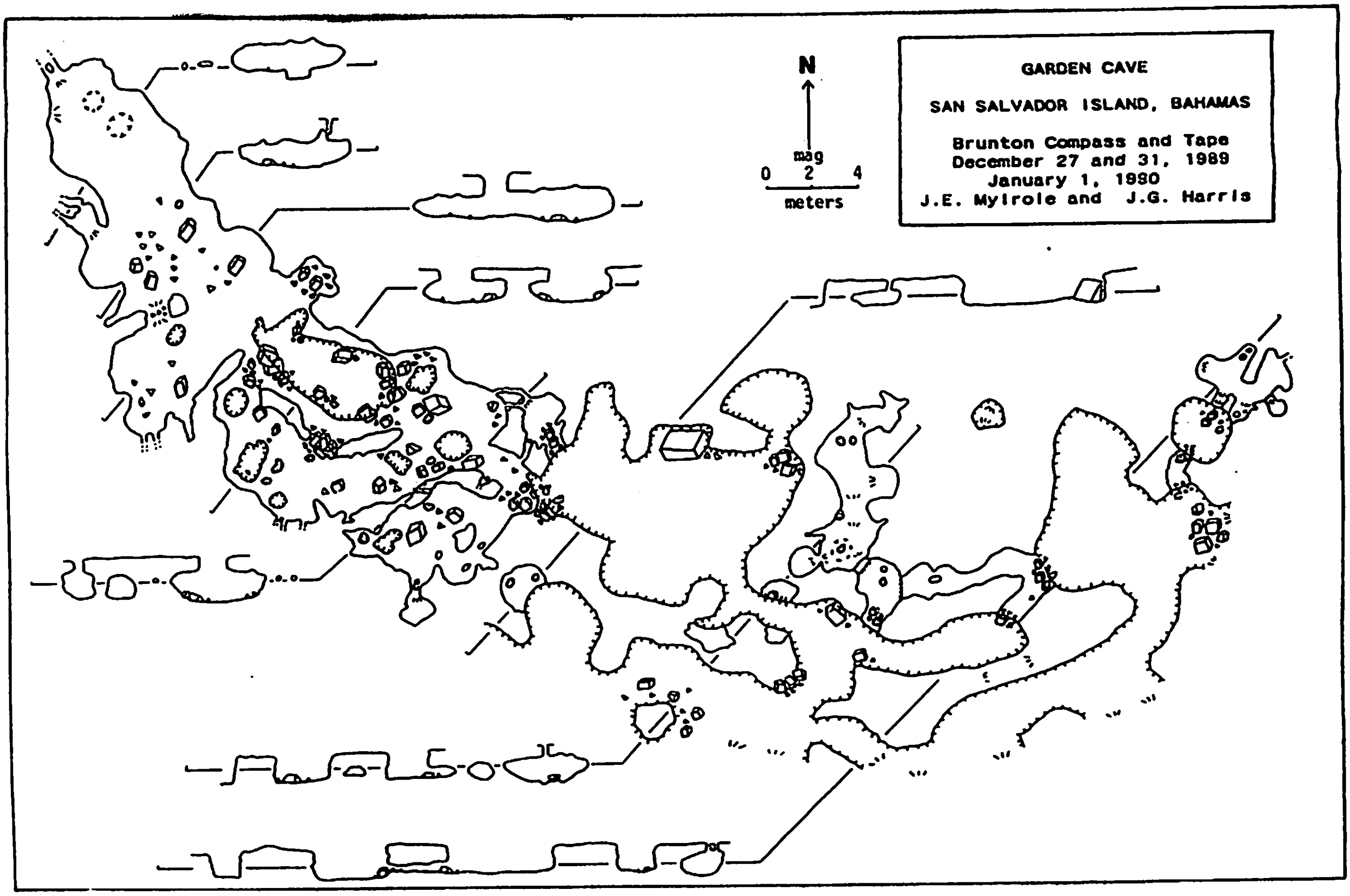

3. Map of Garden Cave, showing passage detail and cross sections.

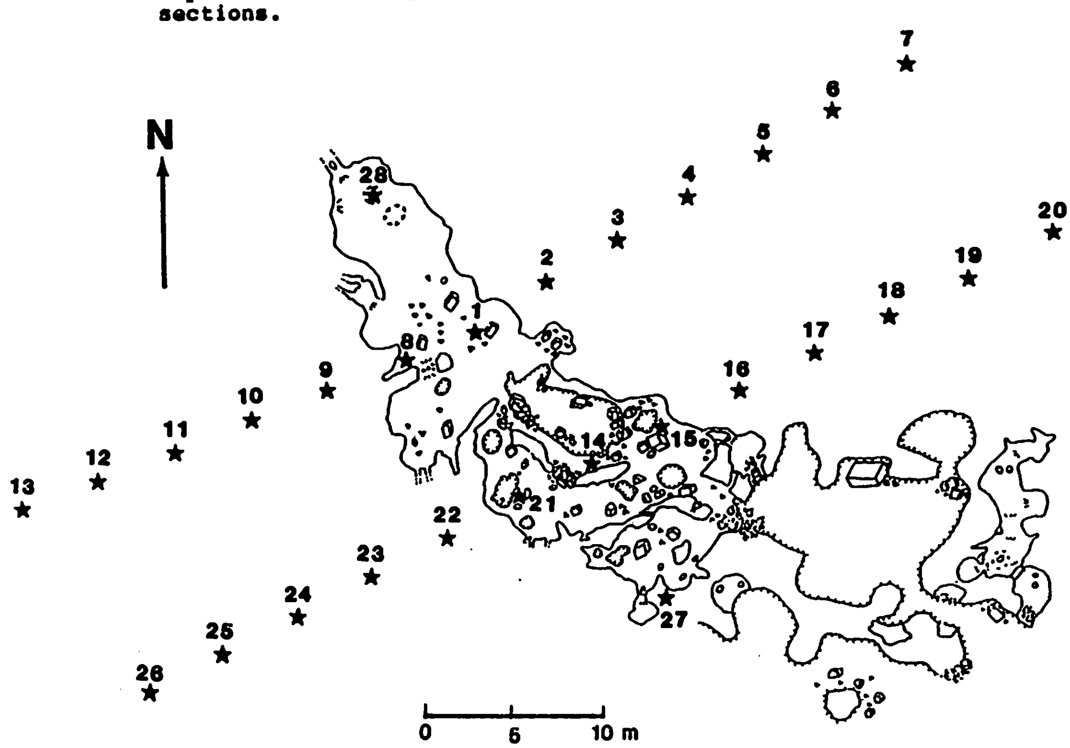

4. Locations of gravity stations with respect to Garden Cave. Stations 1-14 represent Traverse 1, stations 14-26 represent Traverse 2, and stations 27, 14, 1, and 28 comprise a longitudinal profile.

(on different days) for comparison, with similar results. All readings were averaged, normalized to base (station 1) and converted to milligals using the temperature corrected dial constant. The converted readings were corrected for drift (including tides), latitude, and elevation using a rock density of 2.0 g/cm^3. This density corresponds to a porosity (excluding cave passages) of 26%, a value in agreement with earlier porosity determinations of San Salvador near-surface carbonates (Kunze and Weir, 1987; Kunze and others, 1988). Due to the small size of the study area, differential topographic gravity effects are largely negligible (estimated to be less than 10 microgal) and the terrain correction was omitted.The resulting Bouguer anomalies (Figure 5) were filtered by trend surface analysis, utilizing the SYMAP program of the Harvard Laboratory for Computer Graphics, to separate the residual gravity anomaly from the regional trend (dashed lines in Figure 5). The residual anomalies (Figure 7) were compared to theoretical anomalies calculated for the known cave cross sections by two dimensional digital modelling (Figure 8).

RESULTS

The basic data obtained through the microgravity survey are shown as numerical data in Table 1 and the resulting Bouguer anomalies are plotted in Figure 5a (northern traverse), 5b and 5c (southern traverse) and 5d (longitudinal profile). Figure 5c is the 3-point running average of the data in Figure 5b.The corresponding regional trends (dashed lines in Figure 5) were obtained by trend surface analysis as illustrated in Figure 6. Figure 6a is the contour map of the Bouguer anomalies in the study area. Any cave anomaly is masked by a strong SW-NE regional trend in the data. The first order regional trend of all 28 data points is shown in Figure 6b and the corresponding residual gravity anomaly in Figure 6c. This residual map clearly shows the pronounced negative anomaly due to

Table 1: Garden Cave Gravity Data

Station	Elevation (m)	Observed Gravity (mgal)	Bouguer Anomaly (mgal)
1	0	0	0
2	0.47	-0.144	-0.040
3	0.69	-0.194	-0.041
4	0.74	-0.176	-0.013
5	0.85	-0.217	-0.032
6	0.93	-0.230	-0.027
7	1.34	-0.359	-0.067
8	-0.45	0.144	0.044
9	-0.94	0.321	0.112
10	-0.97	0.364	0.150
11	-0.93	0.366	0.162
12	-0.87	0.368	0.176
13	-0.64	0.313	0.175
14	-0.86	0.213	0.023
15	-0.50	0.180	0.071
16	0.10	0.019	0.044
17	0.22	0.024	0.074
18	0.57	-0.147	-0.018
19	0.61	-0.126	-0.010
20	0.72	-0.180	-0.022
21	-1.22	0.370	0.102
22	-1.69	0.561	0.188
23	-1.84	0.672	0.266
24	-1.84	0.627	0.222
25	-1.80	0.616	0.222
26	-1.77	0.666	0.280
27	-1.04	0.335	0.111
28	0.70	-0.197	-0.044

Notes: 1) All data relative to base (station 1)
2) Standard error in gravity readings of +/-0.012 mgal
3) Standard error of Bouguer anomalies is +/- 0.030 mgal

Table 2: Garden Cave Observed And Theoretical Gravity Anomalies

Station	Bouguer Anomaly	Regional Trend	Residual Anomaly	Model Anomaly
1	0	79	-79	-70.3
2	-40	51	-91	-15.0
3	-41	24	-66	-4.0
4	-13	-2	-11	-1.8
5	-32	-28	-4	-1.0
6	-27	-54	27	-0.7
7	-67	-81	14	-0.5
8	44	99	-55	-39.7
9	112	120	-8	-6.8
10	150	141	9	-2.5
11	162	162	0	-1.3
12	176	183	-7	-0.8
13	175	204	-29	-0.6
14	23 (66)*	129	-106 (-63)*	-58.0
15	71 (46)	105	-34 (-59)	-61.7
16	44 (63)	81	-37 (-18)	-5.3
17	74 (33)	57	17 (-24)	-1.9
18	-18 (22)	34	-52 (-12)	-1.0
19	10 (-10)	10	0 (-20)	-0.6
20	-22	-13	-9	-0.4
21	102 (104)	151	-49 (-47)	-45.7
22	188 (186)	175	13 (11)	-5.2
23	266 (225)	198	68 (27)	-1.8
24	222 (237)	222	0 (15)	-1.0
25	222 (242)	246	-24 (-4)	-0.6
26	280	269	11	-0.4

Notes: 1) All anomaly values in microgals
2) *Parentheses values are the three-point running average

5a. Plot of the Bouguer anomaly for Traverse 1. Numbered circles are station locations. Dashed line is regional trend.

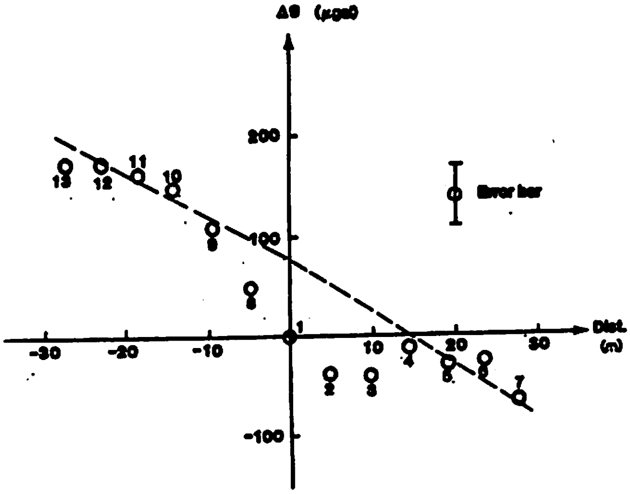

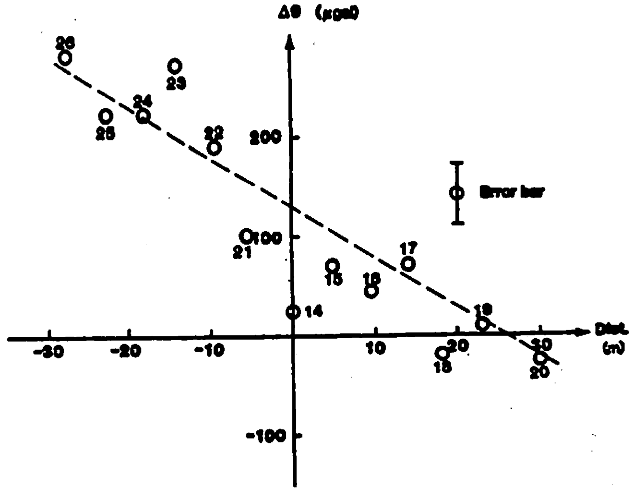

5b. Plot of Bouguer anomaly for Traverse 2. Symbols as in figure 5a.

5c. Plot of Bouguer anomaly for Traverse 2, smoothed with a 3-point running average. Note similarity of this plot with that for Traverse 1. Symbols as in figure 5a.

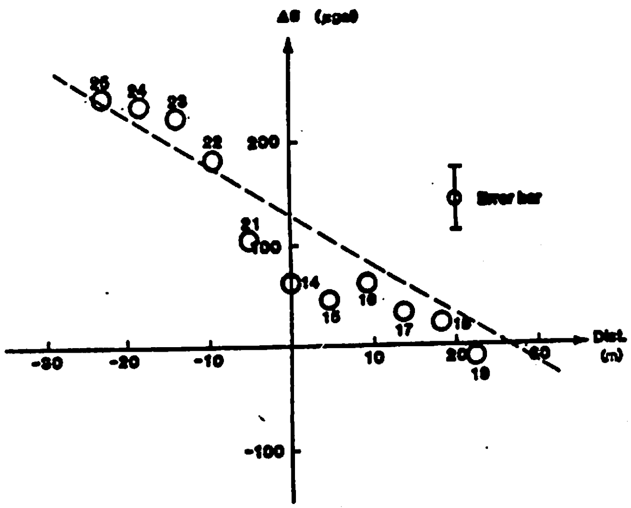

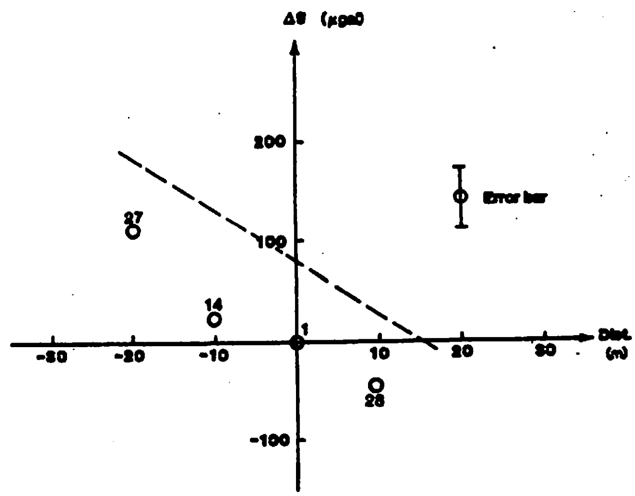

5d. Plot of the Bouguer anomaly for the longitudinal profile. Note that the profile follows the regional trend. Symbols as in figure 5a.

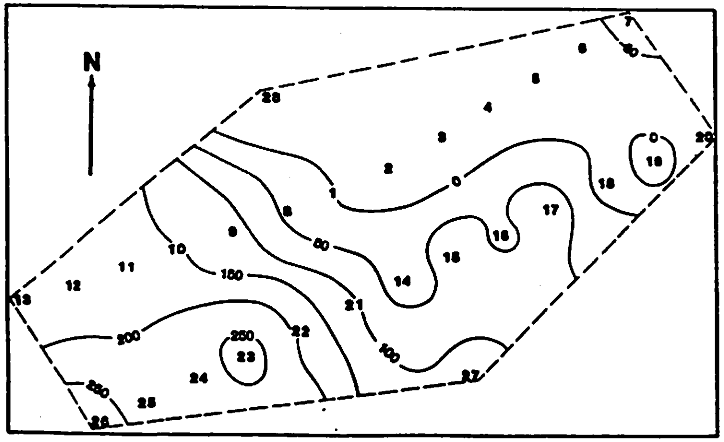

6a. Contour map of the Bouguer anomaly data (see column 4 of Table 1). Contours in microgals, station locations indicated by bold numbers.

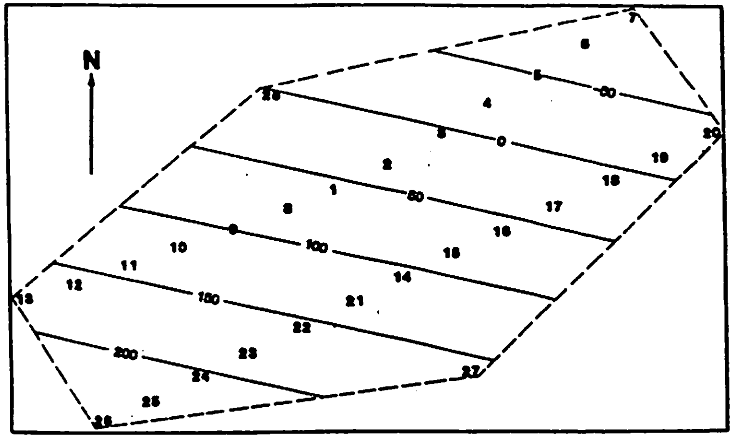

6b. Map of the least-squares first order trend surface of the Bouguer anomaly data (from figure 6a). Symbols as in figure 6a.

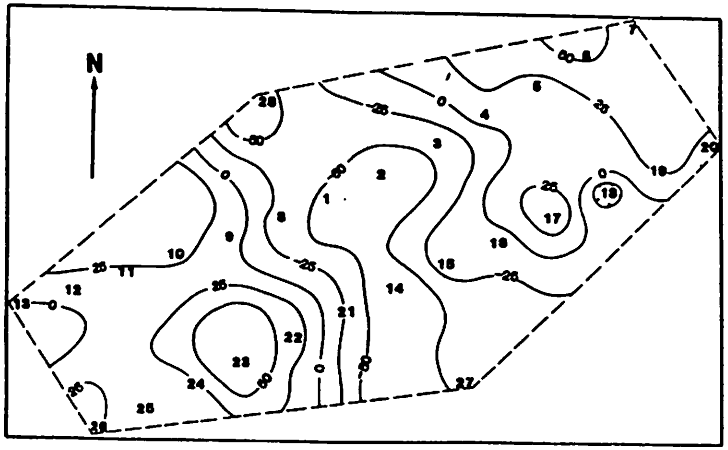

6c. First-order residual Bouguer anomaly map, produced by subtracting data of figure 6b from data of figure 6a. Symbols as in figure 6a.

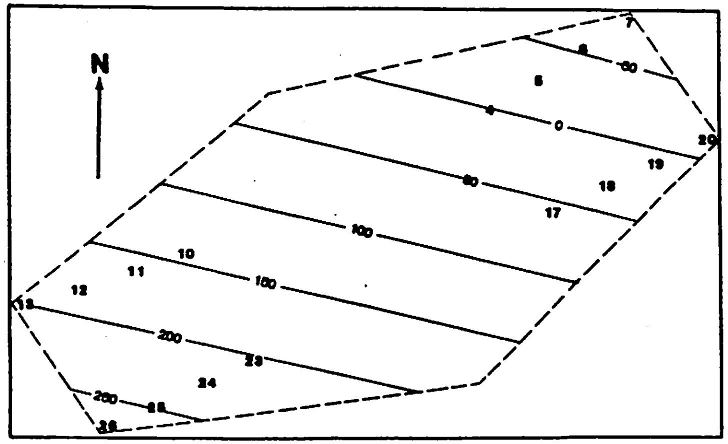

6d. Map of the least-squares first-order trend surface generated from only the 16 outermost stations to remove the influence of Garden Cave from the data. This adjusted trend surface was used to generate the regional trend lines in figures 5. Symbols as in figure 6a.

Garden Cave in the center of the study area. This anomaly, however, is not the true cave anomaly because the regional trend used to define it (Figure 6b) is biased by inclusion of the central anomalous values in the calculation of the least squares first order trend. Figure 6d is a less biased regional trend based on the 16 marginal data points not influenced measurably by the gravity effect of the cave. This more realistic regional trend is shown by the dashed lines of Figure 5. The noticeable change in direction of the regional trend line in Figure 5a is caused by the fact that traverse 1 changes direction at station 1.

The true residual anomalies obtained by subtracting this unbiased regional trend from the Bouguer anomalies are listed in Table 2 and plotted in Figure 7. As before, Figure 7c is the smoothed (by 3-point running average) version of Figure 7b.

Figure 8 shows the theoretical gravity anomalies due to Garden Cave calculated from the two-dimensional gradicule grid patterns representing the known cave cross-sections in the vicinity of traverses 1 and 2. In this calculation the gravity effect of each grid cell (Δgi) is approximated by that of a line element through its center such that

$$\Delta gi = 2G\rho Az/r$$

where G, ρ, A, z, and r are the international gravity constant, element density, cross-sectional area, depth, and slant distance from the observer (station), respectively. The total anomaly at a given station location is the sum of the contributions from all elements. Experimentation with different grid patterns and grid element sizes show the chosen pattern to yield reliable results. The resulting synthetic anomalies shown are corrected for the departure of traverses 1 and 2 from a direction at right angles from the cave trend. The computed synthetic anomalies are also shown on Figure 7 (crosses) for comparison with observed residual anomalies.

Errors

The scatter in the repeated gravimeter readings corresponds to an average standard error in the calculated gravity values (column 3 in table I) of $\pm$0.012 mgal. Station elevations were determined to within $\pm$5cm or less. This uncertainty in elevation leads to an uncertainty in the elevation correction (combined Bouguer and Free-air correction) of no more than $\pm$0.011 mgal. Additional lesser uncertainties arise from unknown density variations and the omission of the terrain correction. Thus, the total standard error in the calculated Bouguer anomalies is estimated to be on the order of $\pm$0.03 mgal or $\pm$30 microgal. This standard error is shown by error bars in Figures 5 and 7.

DISCUSSION

The strong NNE regional gravity trend may be partly caused by a general bedrock density decrease in that direction, underlying platform geology, by the existence of substantial cavities at depth beyond the study area in that direction, or by the generally lower topography beyond Reckley Hill. A minor contribution to this regional trend is also made by the topographic gravity effect of Reckley Hill.

The pattern of the residual gravity anomalies permits more definite interpretations. The gravity effect of Garden Cave is clearly visible in Figures 6c and 7. Comparison of the observed residual anomalies with the synthetic anomalies corresponding to the appropriate known cross-sections of Garden Cave (crosses in Figure 7) shows excellent agreement (well within the error bar) for traverse 2 and the western section of traverse 1, but there is a significant misfit between observed and synthetic gravity data (greater than the error bar) in the eastern section of traverse 1. The observed anomalies there are more negative than those that could be possibly caused by the known portions of Garden Cave. This observation and the anastomosing nature of known flank-margin caves suggests the possibility of another large shallow chamber existing to the northeast of Garden Cave.

One of the many possible hypothetical cave configurations capable of accounting for the observed gravity deficit is shown in Figure 9. The synthetic gravity anomaly (crosses) due to the combined effects of Garden Cave and the hypothetical "Fantasy Cave" matches the gravity observations, supporting this possibility. A small solution pit in that area was subsequently found to lead into a cave chamber of unknown dimensions. The pit, unfortunately, was too small for human entry. Hence, the true size and configuration of "Fantasy Cave" remains unknown.

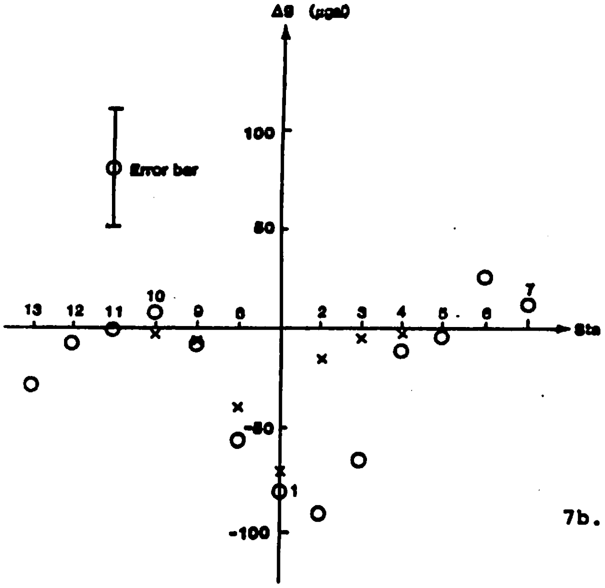

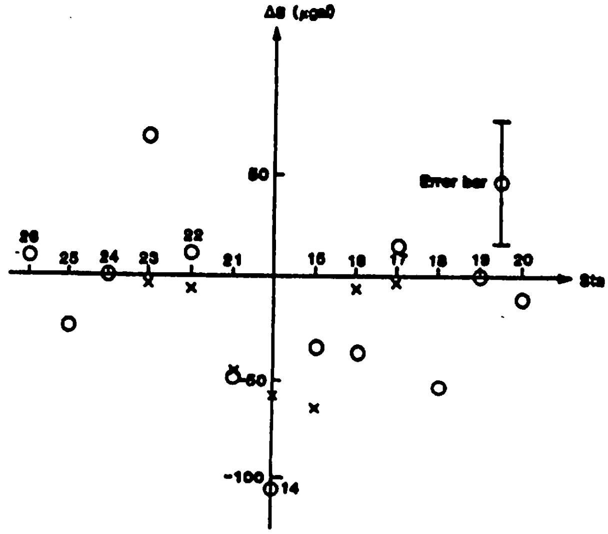

7b. Plot of the residual anomalies of Traverse 2. Conditions the same as for figure 7a.

7a. Plot of the residual anomalies of Traverse 1, produced by subtracting the trend surface values of figure 6d from the Bouguer anomalies of Table 1. Circles are the residual anomalies, crosses are the computed synthetic anomalies based on the 2-D models of figure 8. See also table 2.

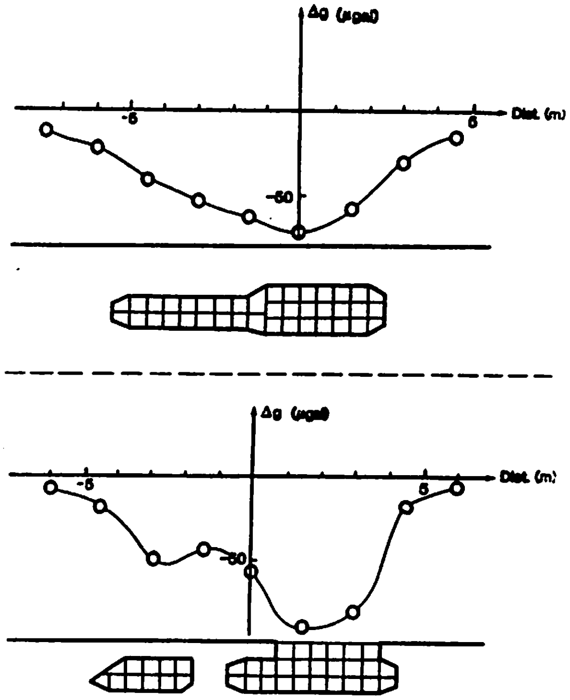

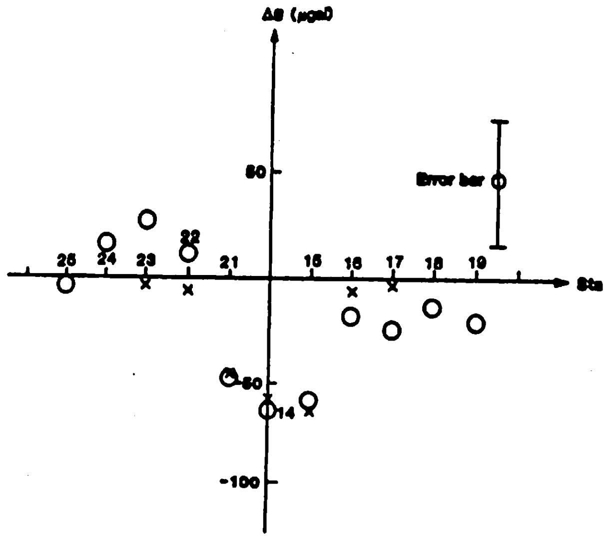

7c.

Plot of the residual anomalies of Traverse 2, smoothed with 3-point running average. Other conditions are the same as for figure 7a.

3. Theoretical gravity anomalies due to approximate 2-dimensional cave cross sections in the regions of Traverses 1 and 2.

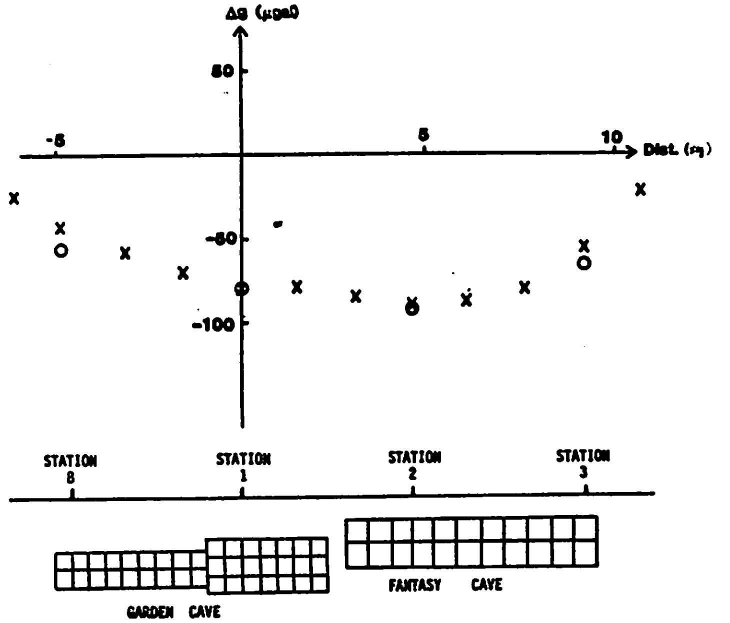

9. Plot of observed (circles) and hypothetical (crosses) anomalies along Traverse 1. The data strongly suggest an undiscovered cave passage, here labelled "Fantasy Cave".

CONCLUSIONS

Gravity survey techniques can be used to locate abandoned flank margin-type dissolution caves in the Bahamas. The dense bush of the Bahama Islands make it impractical to use gravity surveys as a general reconnaissance tool. The technique would seem to have the most value when used in specific localities, such as construction sites, where the nature of the underlying bedrock is critical to site engineering. The shallowness of the flank margin caves makes them readily apparent as a gravity anomaly. Deeper caves, now water-filled, would be much harder to detect because of both the depth factor, and the lower density contrast produced by water-filled conditions.

ACKNOWLEDGMENTS

The authors wish to thank the Executive Director of the Bahamian Field Station, Dr. Donald T. Gerace, for support of this project. Jonathan Harris and Craig Hartline assisted in the collection of field data under difficult conditions; their efforts are appreciated.

REFERENCES CITED

Carew, J. L. and Mylroie, J. E., 1987, A refined geochronology for San Salvador Island, Bahamas: in Curran, H. A., ed., Proceedings of the Third Symposium on the Geology of the Bahamas: CCFL Bahamian Field Station, Fort Lauderdale, FL, p. 35-44.

Kunze, A. W. G. Sauter, A. K. and Weir, W. G., 1989, Geoelectrical Survey of the Columbus Landings I region of San Salvador, Bahamas: in Mylroie, J. E., ed., Proceedings of the Fourth Symposium on the Geology of the Bahamas: Bahamian Field Station, Port Charlotte, FL p. 191-202.

Lundberg, J., 1990 (abstract), Sea-level change over the last 300,000 years in the Bahamas as indicated by submerged flowstone: GEO2, v. 17, nos. 2-3, p. 76.

Mylroie, J. E., 1988, Field Guide to the Karst Geology of San Salvador Island, Bahamas: Bahamian Field Station, Port Charlotte, FL, 108 p.

Mylroie, J. E. and Carew, J. L., 1988, Solution conduits as indicators of Late Quaternary sea level position: Quaternary Science Reviews, v. 7, p. 55-64.

Mylroie, J. E. and Carew, J. L., 1990, The flank margin model for dissolution cave development in carbonate platforms: Earth Surface Processes and Landforms, v. 15, p. 413-424.

Shackleton, N. J. and Opdyke, N. D., 1973, Oxygen isotope and paleomagnetic stratigraphy of equatorial Pacific core V28-238: Oxygen isotope temperatures and ice volumes on a 105 and 106 Scale: Quaternary Research, v. 3, p. 39-55.

Vacher, H. L. and Hearty, P., 1989, History of stage 5 sea level in Bermuda: Review with new evidence of a brief rise to present sea level during substage 5A: Quaternary Science Reviews, v. 8, p. 159-168.

Vogel, P. N., Mylroie, J. E., and Carew, J. L., 1990, Limestone petrology and cave morphology on San Salvador Island, Bahamas: Cave Science, v. 17, no. 1, p. 19-30.

Weir, W. G. and Kunze, A. W. G., 1988, Geoelectrical properties of selected rock and water samples from San Salvador Island, Bahamas: Bulletin of the Association of Engineering Geologists, v. 25, p. 257-263.